

AD-A094 305

CALIFORNIA UNIV LOS ANGELES CENTER FOR PLASMA PHYSIC--ETC F/6 20/9  
GENERATION AND COLLAPSE OF LANGMUIR SOLITONS IN A NONUNIFORM PL--ETC(U)  
NOV 80 N R PEREIRA, G J MORALES N00014-75-C-0476  
PPG-529 NL

UNCLASSIFIED

for  
AD-A094 305



END  
DATE  
FILMED  
13 DEC 80  
DTIC

AD A094305

THE COPY

CENTER FOR  
PLASMA PHYSICS  
AND  
FUSION ENGINEERING

UNIVERSITY OF CALIFORNIA  
LOS ANGELES

12 18 025

(6) Generation and Collapse of Langmuir Solitons

in a Nonuniform Plasma ,

(10) N. R. Pereira and G. J. Morales

(17) PPG-529

(11) November 1980

(15) Contract N00014-75-C-0476

(12) 29

✓  
Letter on file

A  
412152

2/11

# ABSTRACT

This numerical study considers the effect of a zero order density gradient on the development of Langmuir wave collapse in two dimensions. Two different situations are considered: 1) an initial soliton is perturbed in a direction transverse to the density gradient, and 2) the plasma is resonantly driven by an external pump electric field in the presence of transverse density fluctuations. The principal finding is that the density gradient can inhibit the development of Langmuir collapse for both the initial soliton and the externally driven cases. Over the limited parameter space surveyed it is found that collapse occurs for values of the scaled gradient parameter  $g \lesssim 2.5$ ; where  $g = (9/8) (M/m)^{3/2} (\lambda_D/L)$ ,  $M$  is the ion mass,  $m$  the electron mass,  $\lambda_D$  the Debye length, and  $L$  the gradient scale length. For larger values of  $g$  collapse is not observed.

41

to the  $3/2$  power

lambda sub D

less than R  
equal to

p-1

## I. Introduction

The dynamics of the two dimensional collapse of Langmuir waves in uniform plasmas has been extensively investigated over the past few years.<sup>1-4</sup> The collapse process consists of the unbounded localization of the high frequency electric field of a Langmuir wave inside a density cavity of ever increasing depth and decreasing spatial extent. The density cavity is nonlinearly generated by the ponderomotive force produced by the high frequency field. As is well known, in one dimensional plasmas the collapse process does not occur. In this case, a steady state can be obtained in which the dispersion (i.e., the finite group velocity of the wave) exactly balances the nonlinear localization, and a soliton is formed. However, in two dimensions the dispersion is not sufficiently strong to overcome the nonlinearity, and a secular growth of the field with the accompanying density cavity occurs. Since the collapse process arises due to a fluid nonlinearity, i.e., a rearrangement of the electric field energy in wave number space, in an actual plasma the secular growth is limited by kinetic processes (e.g., Landau damping) not retained in the simplified fluid description. Therefore, a possible fate of the collapse process is to transfer the electric field energy of an extended Langmuir wave into kinetic energy of the plasma ions and electrons.<sup>5,6</sup> Consequently, it is of interest to find under what conditions the collapse process occurs and what limitations must be overcome for its onset.

Although several studies have been made of the propagation properties of Langmuir solitons in a one dimensional density gradient,<sup>7-10</sup> to our knowledge, all previous theoretical and numerical studies of two dimensional collapse have considered zero order uniform plasmas.<sup>3,11-18</sup> While this is an interesting simple environment in which to study the basic process, its

applicability to a laboratory plasma is not ensured because such plasmas always have a finite density gradient. The present numerical study is concerned with some aspects of the effect of a density gradient on the collapse process, and the delineation of the threshold conditions required for the experimental observation<sup>19</sup> of this process.

An important and useful feature associated with the density gradient is that it permits the linear generation of localized electric fields at selected points along the density gradient. This excitation can be experimentally attained by applying an external pump field at a frequency  $\omega$  equal to the local plasma frequency  $\omega_p$  of the selected location along the gradient. The external pump drives the local plasma resonance and creates a large localized field which provides a controllable initial condition for the experimental investigation of Langmuir wave collapse. In addition, the consideration of Langmuir wave collapse in a nonuniform plasma and in the presence of an external pump is of interest in connection with the rippling of the resonance absorption surface in laser fusion targets and possibly in future ionosphere modification experiments.

An important effect encountered in a nonuniform plasma is the intrinsic convection of the Langmuir wave energy down the density gradient.<sup>7</sup> Near the  $\omega = \omega_p$  point this convection occurs at a speed roughly given by  $(3/2) \bar{v} (3k_D L)^{-1/3}$ , where  $\bar{v}$  is the electron thermal velocity,  $k_D$  is the Debye wavenumber and  $L$  is the scale length of the gradient. This linear process provides a spreading effect which reduces the effect of the nonlinearity and can prevent the two-dimensional collapse. Therefore, it is of interest to find the threshold condition, i.e., the critical density scale length  $L$  required for the onset of collapse. The present study focuses on this issue for two cases: 1) a pure soliton initial condition, and 2) an externally driven plasma. For the typical numerical cases studied it is found that the collapse process does not occur

for values of the scaled gradient length parameter  $g > 2.5$ ; where,  $g = (9/8) (M/m)^{3/2} (\lambda_D/L)$ ,  $M$  is the ion mass,  $m$  the electron mass, and  $\lambda_D$  the Debye length.

The manuscript is organized as follows. In Sec. II the mathematical model is reviewed and the geometry of the problem is described. Section III discusses the results for the pure soliton initial condition, while in Sec. IV the behavior in the presence of an external pump is presented. A discussion of the results is given in Sec. V.

## II. Mathematical Model

In the present investigation the behavior of the plasma is described by the warm fluid approximation,<sup>1</sup> i.e., wave-particle interactions (e.g., Landau damping, ion acceleration) are neglected. These kinetic effects are not important during the early stage of the collapse process of interest to this study. In the late stage of the collapse process strong energy absorption occurs due to electron transit time damping. The description of such an effect is beyond the scope of this work. In addition, high frequency electron nonlinearities, such as second harmonic generation, are neglected because they give rise to oscillations which are not normal modes of the plasma. Also, corrections to the ion acoustic wave due to ion nonlinearities are not included.

The high frequency electric field  $\vec{E}_h$  is described through a modulational representation

$$\vec{E}_h = \vec{E}(x, y, t) \exp(-i\omega_p t) + c.c. \quad (1)$$

where  $x$  is the spatial direction along the density gradient and  $y$  is perpendicular to  $x$ . The time dependence of the complex vector amplitude  $\vec{E}$  is assumed to be slow compared to a plasma period, i.e.,

$$\left| \frac{\partial^2 \vec{E}}{\partial t^2} \right| \ll \omega_p^2 |\vec{E}| \quad (2)$$

so that only the first order time derivative is retained in the two-dimensional evolution equation

$$\nabla \cdot \left\{ \frac{2i}{\omega} \frac{\partial \vec{E}}{\partial t} + 3\lambda_D^2 \nabla (\nabla \cdot \vec{E}) - \left( \frac{\tilde{n}}{n_0} + \frac{x}{L} \right) \vec{E} - \vec{E}_p \right\} = 0 \quad (3)$$

where  $\tilde{n}$  refers to the nonlinearly generated low frequency density fluctuation, and  $n_0$  is the plasma density at the point  $\omega_p = \omega$  along the gradient.



The external pump field  $\vec{E}_{p,h}$  of frequency  $\omega$  is assumed to be of the capacitor type (i.e., near field) and is represented by

$$\vec{E}_{p,h} = E_p \exp(-i\omega t) \hat{x} \quad (4)$$

where  $E_p$  is the constant strength and  $\hat{x}$  is the unit vector in the  $x$  direction. The zero order density profile is taken to be linear, with characteristic scale length  $L$ , i.e.,

$$1 - \frac{\omega_p^2}{\omega^2} = - \frac{x}{L} \quad (5)$$

The density fluctuations are determined self-consistently from the two-dimensional linearized ion-acoustic wave equation in which the ponderomotive force due to the high frequency field plays the role of a source, i.e.,

$$\left( \frac{1}{c_s^2} \frac{\partial^2}{\partial t^2} - \nabla^2 \right) \left( \frac{\tilde{n}}{n_0} \right) = \nabla^2 \left( \frac{|\vec{E}|^2}{16\pi n_0 T} \right) \quad (6)$$

where  $c_s$  is the ion sound speed, and  $T$  the electron temperature.

The coupled equations (3) and (6) form the mathematical description of the problem. It should be noted that in this formulation the full vector character of the electric field is retained, as well as the effect of ion inertia.

In scaling the physical variables appearing in Eqs. (3) and (6) one encounters two choices: (1) scaling according to the Airy-like scaling associated with the density gradient,<sup>7</sup> or 2) scale according to the slow time response of the ions as is done in the collapse studies in uniform plasmas.<sup>1,3,11-18</sup> In this work we have chosen the latter scheme in order to retain contact with the previous collapse literature as well as with the results obtained with the earlier version<sup>3</sup> of the computer code used to solve Eqs. (3) and (6).

Using the scaled variables  $\xi = x/x_s$ ,  $\eta = y/x_s$ ,  $\tau = t/t_s$ ,  $\vec{E} = \vec{E}/E_s$ ,  $N = \tilde{n}/n_s$ , where

$$\begin{aligned} x_s &= (3/2)(M/m)^{1/2} \lambda_D, \quad t_s = (3/2)(M/m) \omega_p^{-1} \\ n_s &= (4/3)(m/M) n_0, \quad E_s = (64\pi n_0 m c_s^2 / 3)^{1/2} \end{aligned} \quad (7)$$

results in the scaled equations

$$\nabla \cdot \left\{ i \frac{\partial}{\partial \tau} \vec{E} + \nabla (\nabla \cdot \vec{E}) - (N + g\xi) \vec{E} - E_p \hat{x} \right\} = 0 \quad (8)$$

$$\left( \frac{\partial^2}{\partial \tau^2} - \nabla^2 \right) N = \nabla^2 |\vec{E}|^2 \quad (9)$$

in which two lumped parameters appear. The parameter  $g$  given by

$$g = (9/8) (M/m)^{3/2} (\lambda_D/L) \quad (10)$$

measures the relative sharpness of the density gradient, while the parameter

$E_p$  defined by

$$E_p = [(3)^{3/2}/16] (M/m)^{3/2} [E_p / (4\pi n_0 T)^{1/2}] \quad (11)$$

describes the strength of the external pump.

It is clear from the definitions in Eqs. (10) and (11) that the present choice of scaling is optimum for long scale length profiles, (i.e., weak nonuniformity) and small external pumps. When  $L$  is decreased and/or  $E_p$  is increased a more appropriate scaling for this problem is the Airy-like scaling. In the Airy scaling one still has two lumped parameters,  $p$  and  $V^2$ , which uniquely determine the behavior of the system. The parameter  $p = (k_D L)^2 E_p^2 / 12\pi n_0 T$

measures the degree of nonlinearity, while  $V^2 = (4/3)(M/m)(k_D L/\sqrt{3})^{-2/3}$  accounts for the relative role of ion inertia in the formation of the density cavities. In transforming these parameters from one scaling to the other obtains  $p = (32/9)(\mathcal{E}_p/g)^2$ ,  $V = (4/3)g^{1/3}$ . From this relationship it is seen that for large values of  $g$  and  $\mathcal{E}_p$  the Airy scaling is more convenient because both  $p$  and  $V$  can remain of order unity. For values of  $g$  and  $\mathcal{E}_p$  of order unity, the two descriptions are equally useful, while for  $g$  very small (i.e., uniform plasmas) the scaling given in Eq. (7) is more appropriate. In either choice of description, it should be stressed that the real physical problem has three independent parameters,  $(M/m)$ ,  $(k_D L)$  and  $E_p^2/n_o T$ ; however, the response of the system has an internal self-similarity governed only by the two lumped parameters  $(g, \mathcal{E}_p)$  or equivalently  $(p, V)$ .

The parameter space surveyed in the present numerical study has concentrated in the region where the scaling given in Eq. (7) is useful, i.e., both  $g$  and  $\mathcal{E}_p$  are of order unity. However, the values of the parameters chosen differ significantly from those of a recent experiment<sup>19</sup> designed to study two-dimensional resonantly enhanced electric fields. The laboratory gradient scale length  $g$  and the pump field  $\mathcal{E}_p$  are larger than 100 in the present units, therefore our numerical results are not strictly applicable to such an experiment. To describe this experiment one should consider a third scaling, i.e., to the ion time scale,  $t_s = (m/M)^{1/2} \tau$ , and corresponding scalings of space, density and fields.

The numerical method applied to Eqs. (8) and (9) uses the spectral representation for the derivatives, and computes the nonlinear terms at each time step from a Fourier transform to configuration space. The system is periodic in the  $y$ -direction. To accommodate the inhomogeneity term  $-g\mathcal{E}_p$  within the

periodic Fourier method the system is extended the in x-direction by its mirror image, and periodicity is enforced in the doubled system. Typical computational parameters are 32 grid points in y and 32 in x, (64 grid points in the doubled system) with grid spacings  $\Delta\xi = 0.25$ ,  $\Delta\eta = 0.25$ , and time step 0.02. In the late stages of the computation nonzero values of  $|\vec{E}|^2$  and N are sometimes found at the lower boundary in x, thus indicating a finite leakage from the mirror image of the system. It has been found that this leakage does not appreciably change the results, as evidenced by comparisons with calculations in which a damping term at the lower boundary is included in Eq. (8).

### III. Undriven Solitons

Before proceeding to investigate the behavior of Langmuir wave collapse arising from the resonant excitation by an external pump, it is useful to determine first the effect of a density gradient on the collapse process experienced by an initial one dimensional soliton. For this purpose the electric field at  $t = 0$  is

$$\vec{E} = \sqrt{2} \kappa \operatorname{sech}(\kappa \xi) \hat{x} \quad (12)$$

The density perturbation is given by

$$N = -2\kappa^2 \operatorname{sech}^2(\kappa \xi) [1 + \delta \cos(k_y \eta)] \quad (13)$$

and  $\partial N / \partial t = 0$  as in previous numerical studies.<sup>3,15</sup> In Eqs. (12) and (13)  $\kappa^{-1}$  represents the width of the soliton,  $\delta$  the depth of the transverse modulation, and  $k_y$  the scaled transverse wavenumber of the modulation. The field given by Eq. (12) corresponds to a stationary soliton in a one-dimensional plasma without a density gradient, when the nonlinearly modified density is  $N = -|\vec{E}|^2$ . The growth in the transverse direction is triggered by perturbing this value of  $N$  by the expression shown in Eq. (13).

An analytical one-dimensional exact solution of Eqs. (8) and (9) does not seem to exist.<sup>9</sup> However, if ion inertia is ignored, i.e., setting  $N = -|\vec{E}|^2$  in Eq. (8), a linear density gradient can be transformed away by going to an accelerating reference frame,<sup>10</sup> and in this case Eqs. (12) and (13) are the correct initial conditions.

The effect of the density gradient has been examined by solving Eqs. (8) and (9) for different values of the scaled gradient parameter  $g$ . It is found that for  $\kappa = 2$ ,  $\delta = 0.1$ , and  $k_y = 2\pi/16$ , collapse occurs for  $g \leq 2.5$  and its general features are quite analogous to the results obtained for a

uniform plasma. The typical spatial patterns are shown in Fig. 1 for the case  $g = 1$  and a time  $\tau = 1.75$ . In these three dimensional plots, the top part represents the two dimensional  $(\xi, \eta)$  dependence of  $|\vec{\epsilon}|^2$ , while the bottom represents the perturbed density. The development of the transverse modulation is evident in this figure, in which the maximum value of  $|\vec{\epsilon}|^2$  is 40.7 and the deepest portion of the density cavity is  $N = -24.0$ . It should be remembered, however, that the spatial dependence of the total density in the plasma is given by  $N + g\xi$ , so that the cavity seen at the bottom of Fig. 1 is part of a sloping density profile, not shown in this presentation. Notice also the small regions of positive density changes adjacent to the collapsing peak, and the corresponding reduction of  $|\vec{\epsilon}|^2$ .

As the value of  $g$  is increased, it is found that the time required to observe collapse patterns of the type shown in Fig. 1 increases rapidly. For large values of  $g$ , the initial soliton moves rapidly down the density gradient and the transverse perturbation does not have a chance to affect its evolution, i.e., the soliton outruns the transverse modulation. To quantify this behavior it is useful to plot the time evolution of the peak amplitude of the electric field  $|\vec{\epsilon}|_m^2$  for different values of the scaled gradient parameter  $g$ , as shown in Fig. 2. In this figure one observes a continuous transition from a collapse case ( $g = 0$ ) with an asymptotic collapse time  $\tau_c \sim 1.5$  to a nearly constant behavior for  $g = 4$ . For the various cases that we have run it appears that the value of  $g \leq 2.5$  sets the threshold scale for collapse, at least for the perpendicular instability growth rate determined by  $\delta$  and the perpendicular wavenumber  $k_y = 2\pi/16$ . Computations with other perpendicular wavenumbers seem to confirm the obvious generalization: collapse occurs when the streaming of  $|\vec{\epsilon}|^2$  into the perturbed density cavity exceeds the convection of  $|\vec{\epsilon}|^2$  due to the density gradient (see further Section V.)

#### IV. Resonant Pumping

Having established that the collapse of a one dimensional soliton can be quenched by a finite density gradient above a certain threshold value, we proceed to examine the behavior of a plasma in which the field structure is self-consistently determined by an external uniform pump. The pump gives rise to a resonant electric field at  $\omega = \omega_p(x)$  whose peak amplitude is limited, in the small amplitude regime, by the convection of a Langmuir wave down the density gradient. In the one dimensional case, as the amplitude of the pump is increased, density cavities are generated. These cavities give rise to the transient enhancement and localization of the field. However, due to the steady convection down the gradient, the field localization is temporary. Consequently, in this environment one obtains a continuous generation of cavities and localized fields.<sup>7</sup>

One of the issues of interest in this problem is whether or not the regenerative one dimensional localized structures can break-up in the transverse direction, and what the threshold conditions are for this process to occur. In a limited survey of the large parameter space defined by this problem we have found that it is possible to obtain a two-dimensional collapse which arises naturally out of the Airy-like patterns associated with resonant pumping. An example of such a collapse is illustrated in Fig. 3. This figure shows the two dimensional spatial dependence of the electric field  $|\vec{E}|^2$  at  $\tau = 3.75$ . The external pump is turned on suddenly at  $\tau = 0$  with a value of  $\epsilon_p = 1.5$  and the two dimensional collapse is stimulated by providing the plasma with an initial density perturbation given by  $N(\tau = 0) = \delta \cos(k_y \eta) \cos(k_x \xi)$  (i.e., a density bowl with  $\delta = 0.4$ ,  $k_y = 2\pi/16$  and  $k_x = \pi/8$  and again with  $\partial N / \partial \tau = 0$ ).

It should be noted that in Fig. 3 the cold plasma resonance is located at  $\xi = 0$  and that the first peak to its left is not the result of collapse, but rather the typical Airy peak. This peak experiences a weak transverse

modulation, but no major redistribution of the field energy occurs. Instead, for the parameters chosen the collapse occurred on a secondary peak which at a previous time had its origin at the  $\omega_p$  point ( $\xi = 0$ ), but which propagated down the gradient in the manner described at the beginning of this section. The perturbed density associated with the field of Fig. 3 is shown in Fig. 4. A deep cavity of depth  $N = -19.4$  coincides with the peak of the electric field. An interesting feature seen in this picture is the appearance of density compressions between the collapse peak and the normal Airy-like patterns. These are due to the expulsion of ion density from the regions of high electric field, and in particular from the collapse region.

Figure 5 displays the spatial dependence of the total electric field  $|\vec{E}|^2$  and the scaled density profile  $N + g\xi$  along the  $\xi$  direction (i.e., in the gradient direction) for a cut along  $\eta = 0$  corresponding to the transverse location of the peak electric field at  $\tau = 3.75$ . This figure clearly shows the usual flattening of the profile just to the left of the  $\omega_p = \omega$  resonance, and the new feature associated with collapse at  $\xi \approx -4.0$ .

To complement the display in Fig. 5 we exhibit the transverse dependence (i.e., along  $y$ ) in Fig. 6. The two curves shown correspond to constant  $\xi$  cuts passing through the peaks of the total field (solid curve) and the  $\eta$  component of the field  $|\xi_\eta|^2$  (dashed curve). Because of the  $\eta$ -symmetry of the collapse, the peak of  $|\xi_\eta|^2$  cannot occur in the same location as the peak of  $|\vec{E}|^2$ , instead it is located where the derivatives of  $\vec{E}$  are large, i.e., to the side of the collapsing soliton. From Fig. 6 it is clear that the peak value of the  $\xi$  component of the field is considerably larger than the peak value of the  $\eta$  component. However, because these two peaks do not coincide spatially it is possible to find regions in which the two components attain comparable levels. This feature should be kept in mind when interpreting experiments which rely on electron deflection techniques to measure the development of the transverse modulation.



Finally, Fig. 7 exhibits the time evolution of the peak electric field,  $|\vec{E}|_m^2$  and the deepest density cavity  $N_m$ . For early times ( $\tau < 2.5$ ) the growth in the peak electric field is associated with the resonant pumping. During this stage the field pattern is essentially one dimensional. However, for  $\tau > 2.5$  one observes the rapid development of the collapsing field shown in Fig. 3.

In the presence of external pumping the collapse process can also be quenched for  $g \geq 2.5$ . In this regime one finds essentially the continuous generation of peaks and density cavities along the density gradient, as obtained in an earlier one dimensional study.<sup>7</sup>

## V. Discussion

The principal result obtained in this study is that a density gradient can inhibit the development of two dimensional Langmuir wave collapse. The inhibition occurs for initial soliton-like conditions, as well as for the external resonant pumping case. Although the parameter space surveyed has been limited to the neighborhood of  $g \leq 4$ ,  $\epsilon_p < 2$ , and initial field levels  $|\vec{E}(\tau = 0)|^2 \leq 8$ , it is expected that a gradient threshold condition also exists in the large parameter space not sampled. For our parameters the collapse occurs for density length scales such that  $g \leq 2.5$ .

To obtain a semi-quantitative description for the reason behind the threshold, it should be realized that a necessary (but not sufficient) condition for the development of collapse is that the convection down the density gradient should not outrun the transverse growth of the modulation. Mathematically, this implies that  $v_c < v_m$ , where  $v_c = (3/2)\bar{v}(\lambda_D/3L)^{1/3}$  represents the intrinsic convection speed down the gradient. For a rapidly growing transverse modulation, the transverse speed  $v_m$  is determined by the growth rate  $\gamma_m$ , i.e.,  $v_m = \gamma_m/k_y$ , where  $k_y$  is the transverse wavenumber. For initial conditions resembling the cases investigated, the growth rate of the modulation is essentially given by<sup>3,12</sup>

$$\gamma_m \approx (0.4) \left( \frac{k_y}{k_D} \right) \frac{|\vec{E}|}{[(64\pi/3)n_0 T]^{1/2}} \quad (14)$$

which gives rise to the threshold condition

$$(6/\sqrt{2}) (\lambda_D/3L)^{1/3} < (0.4) \frac{|\vec{E}|}{\sqrt{4\pi n_0 T}} \quad (15)$$

This estimate shows that for a fixed  $L$  the initial field must be above a certain level, or alternatively, for a fixed  $|\vec{E}(\tau = 0)|$  there is a minimum value of  $L$  below which collapse does not occur. Using the definition for  $g$  and the scaling described in Eq. (7), the threshold condition in Eq. (15) can be simply put in the form

$$g^{1/3} < (0.4) |\vec{E}| \quad (16)$$

For the typical initial amplitude used in the soliton study,  $|\vec{E}| = \sqrt{8}$ , hence predicting a threshold value of  $g \approx 1.5$ .

To obtain the threshold condition in the presence of an external pump  $E_0$ , the electric field  $|\vec{E}|$  in Eq. (15) should be identified with the resonantly enhanced field inside the plasma, i.e.,  $|\vec{E}| \approx (1.7) (k_D L / \sqrt{3})^{2/3} E_0$ . Solving now for the condition required on  $L$  leads to the expression

$$(3/\pi\sqrt{2}) (\lambda_D/L) < \frac{E_0}{\sqrt{4\pi n_e T}} \quad (17)$$

which can be satisfied for typical laboratory parameters. Clearly, Eqs. (15) and (17) are simple scaling arguments to be used in making rough comparisons. In order to obtain a rigorous threshold a considerably more elaborate analysis is required.

#### Acknowledgements

Stimulating discussions with Professors B. D. Fried, A. Y. Wong, and Mr. D. L. Eggleston are gratefully acknowledged. This work was sponsored by NSF under contract 4-444024-21508-3 and the Office of Naval Research.

### References

1. V. E. Zakharov, Zh. ETF, 62, 1745 (1972) [Sov. Phys. JETP 35, 908 (1972)].
2. V. Makhankov, Phys. Reports, 35C, 1 (1978), and references therein.
3. N. R. Pereira, J. Denavit, and R. N. Sudan, Phys. Fluids, 20, 936 (1977).
4. M. V. Goldman, K. Rypdal and B. Hafizi, Phys. Fluids, 23, 945 (1980).
5. N. R. Pereira, J. Denavit, and R. N. Sudan, Phys. Fluids, 20, 271 (1977).
6. H. P. Freund, I. Haber, P. Palmadesso, and K. Papadopolous, Phys. Fluids, 23, 518 (1980).
7. G. J. Morales and Y. C. Lee, Phys. Fluids, 20, 1135 (1977).
8. A. Bondeson, Phys. Fluids, 23, 746 (1980).
9. K. H. Spatschek and E. W. Laedke, Proceedings of the International Plasma Physics Conference, Nagoya, Japan 1980 (Paper 10 P-II-13).
10. H. H. Chen and C. S. Liu, Phys. Fluids, 21, 337 (1978).
11. V. E. Zakharov and A. M. Rubenchik, Zh. TEF 65 997 (1973), [Sov. Phys. JEPT 38, 494 (1974).]
12. L. M. Degtyarev, V. E. Zakharov, and L. I. Rudakov, Zh. TEF, (Sov. Phys. JEPT 41, 57 (1975)].
13. N. Yayima, Prog. Theor. Phys. 52, 1006 (1974).
14. G. Schmidt, Phys. Rev. Lett. 34, 724 (1975).
15. M. J. Wardrop and D. Ter Haar, Phys. Scripta, 20, 493 (1979).
16. D. Anderson, A. Bondeson and M. Lisak, Phys. Scripta 20, 343 (1979).
17. M. V. Goldman and D. W. Nicholson, Phys. Rev. Lett., 41, 406 (1978).
18. E. W. Laedke, and K. H. Spatschek, Phys. Fluids 23, 44 (1980).
19. D. L. Eggleston, A. Y. Wong, and B. C. Darrow, UCLA Plasma Physics Report, PPG-506, to be published.

FIGURE CAPTIONS

- Fig. 1 Two dimensional spatial dependence of the scaled electric field energy density  $|\vec{E}|^2$  (top) and scaled density change  $N$  (bottom) for  $g = 1.0$  at  $\tau = 1.75$ . The peak values are  $|\vec{E}|_m^2 = 40.7$  and  $N_m = -24.0$ .
- Fig. 2 Time evolution of the peak amplitude of the scaled electric field  $|\vec{E}|_m^2$  for different values of the scaled density gradient;  $g = 0$  corresponds to a uniform plasma.
- Fig. 3 Two dimensional spatial dependence of the electric field energy density  $|\vec{E}|^2$  obtained in the presence of an external pump  $E_p = 1.5$  at  $\tau = 3.65$  and  $g = 1.5$
- Fig. 4 Density perturbation corresponding to Figure 3.
- Fig. 5 Spatial dependence of the electric field energy density  $|\vec{E}|^2$  along the zero order density gradient for the case of Fig. 3. The dashed curve corresponds to the scaled density profile.
- Fig. 6 Spatial dependence in the direction transverse to the density gradient.  $|\vec{E}|^2$  is the total energy density and  $|E_n|^2$  is the contribution of the  $n$  component. Curves are obtained along constant  $y$  values passing through the respective maximum.
- Fig. 7 Time evolution of the peak amplitude of the scaled electric field  $|\vec{E}|_m^2$  and deepest scaled density cavity in the presence of an external pump  $E_p = 1.5$ ,  $g = 1.5$ .

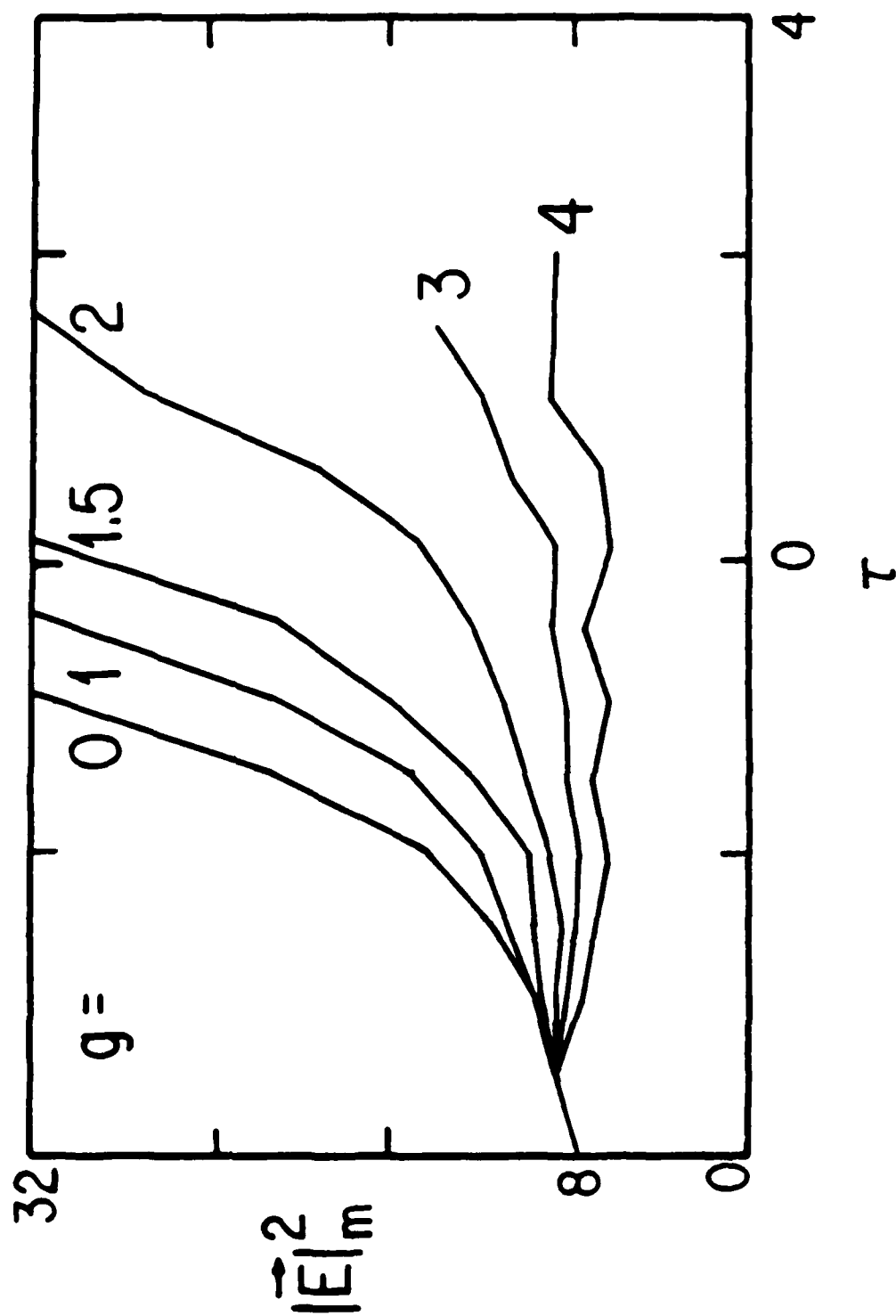


FIG. 2

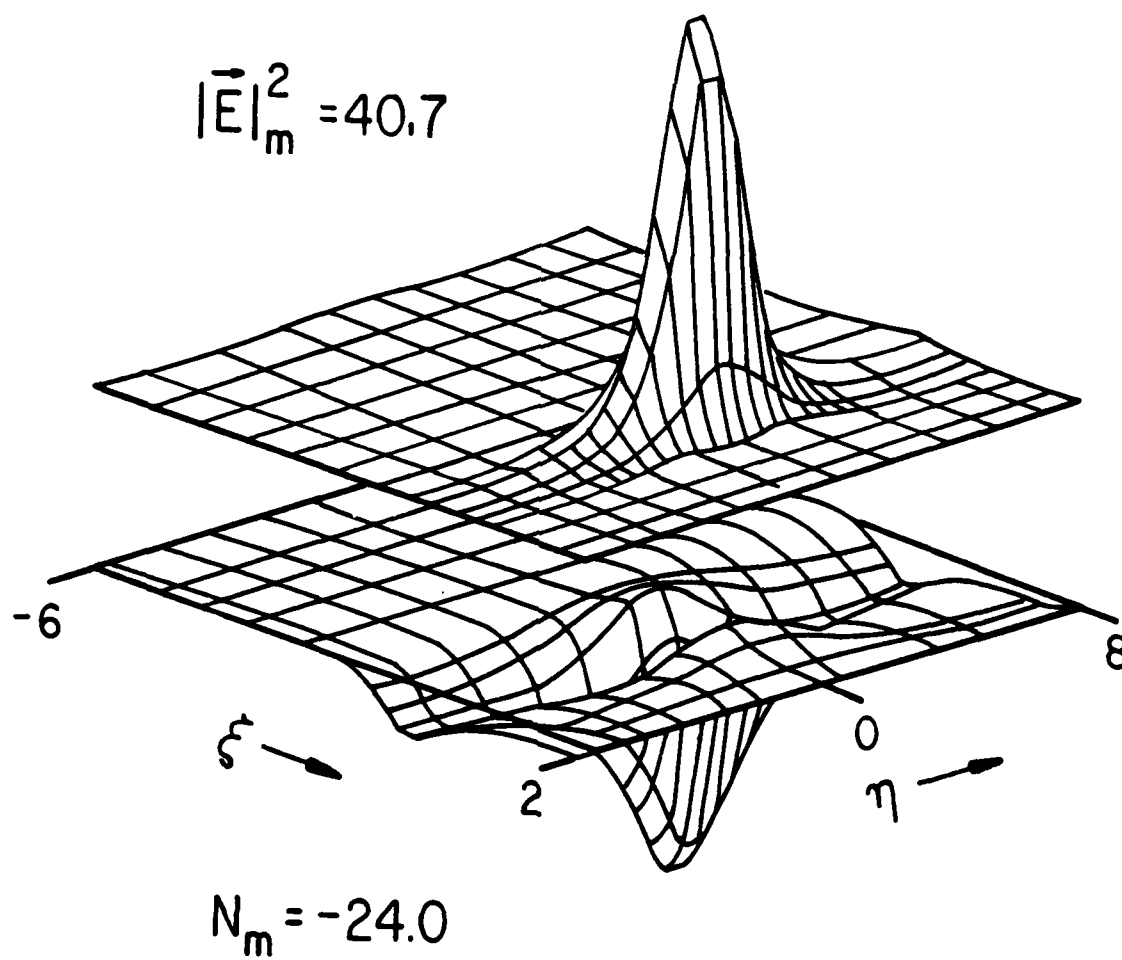


FIG. 1

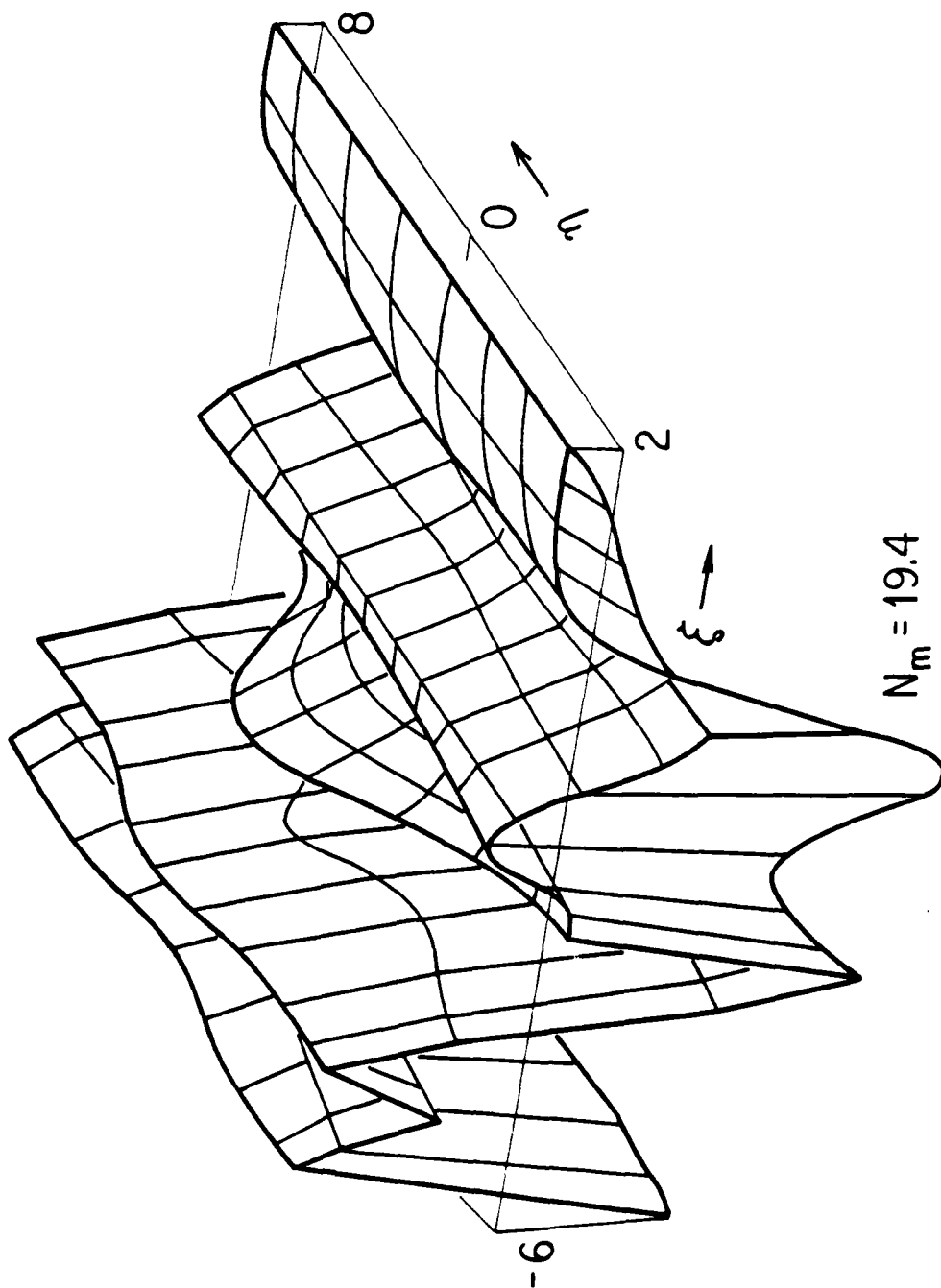


FIG. 4



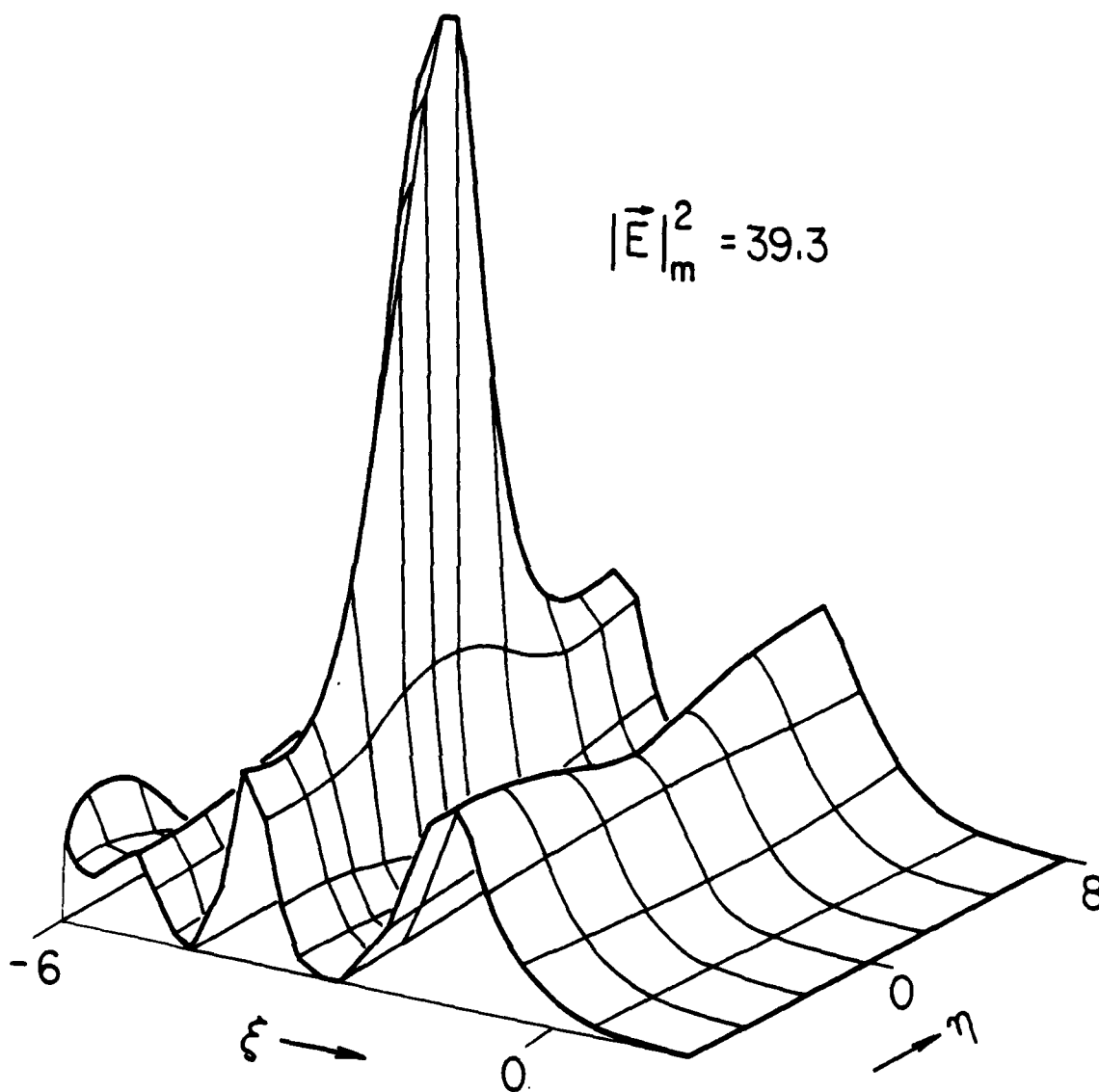


FIG. 3

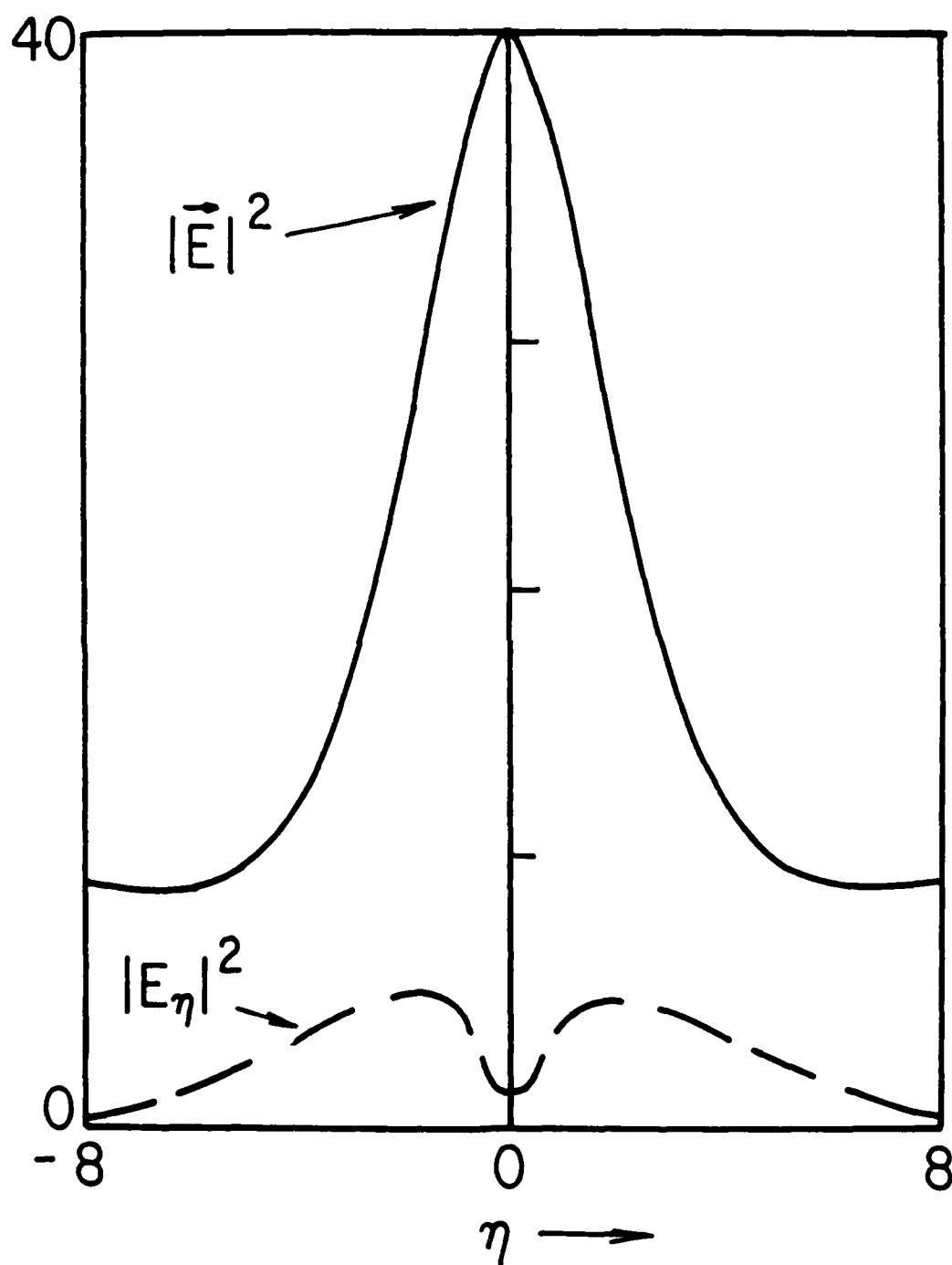


FIG. 6

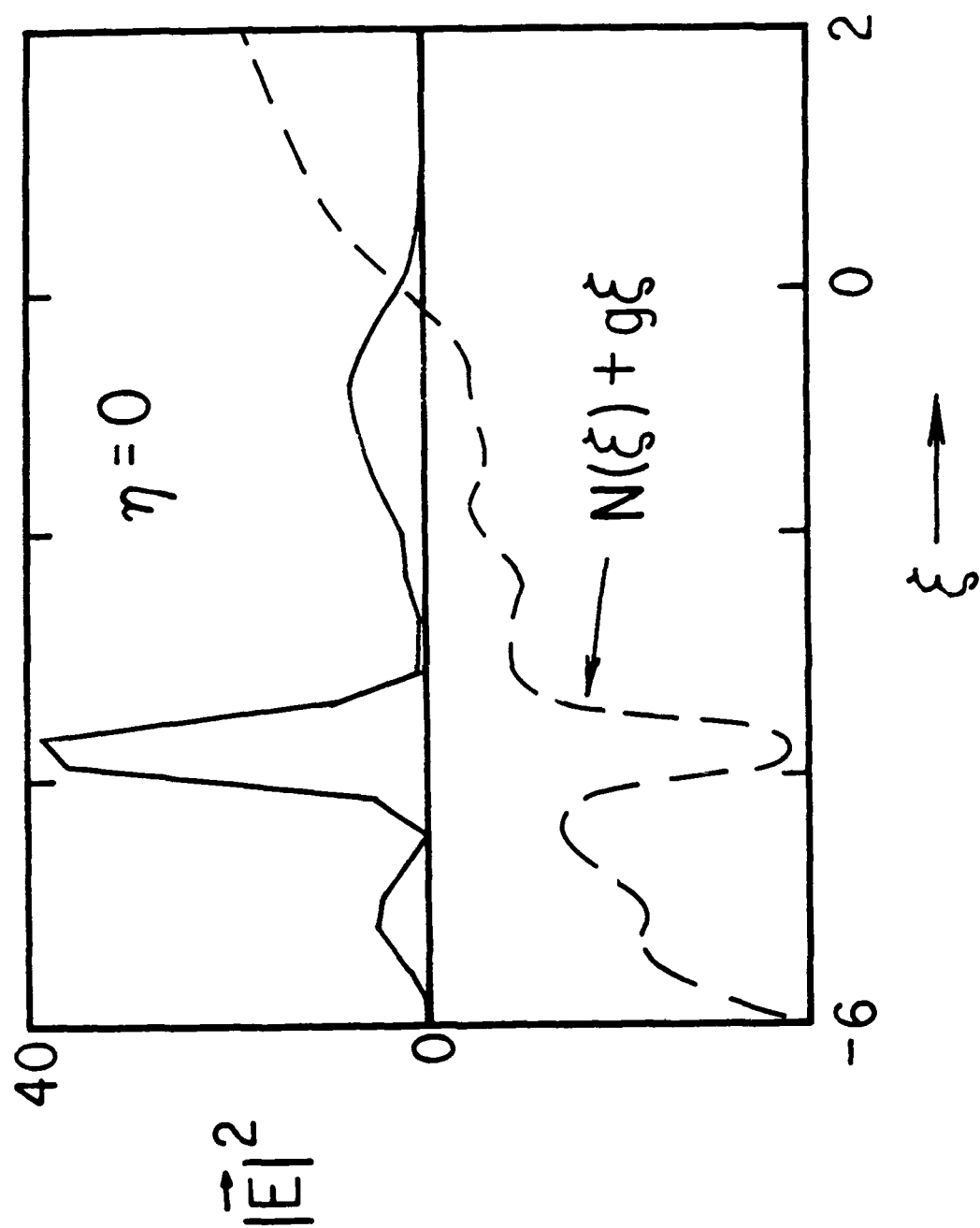


FIG. 5

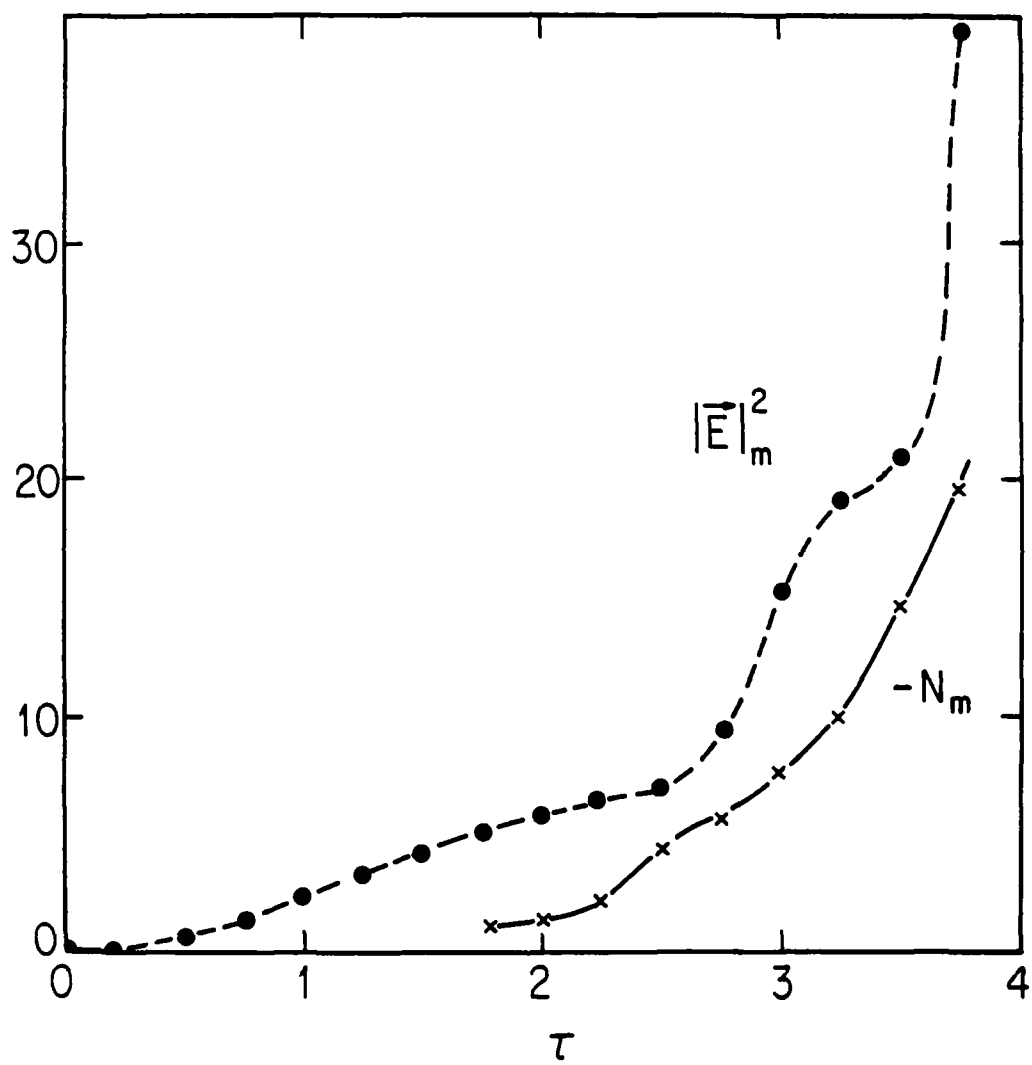


FIG. 7

- PPG-495 "Quartz Crystal Oscillator Stickness Monitor in In-Situ Wall Coatings in Macrotor and Microtor Tokamaks," E. M. Tenescu and R. J. Taylor, June (1980).
- PPG-496 "Effect of Finite Electron Drift Velocity on the Resonant Excitation of a Nonuniform Plasma," G. J. Morales, B. N. Lamb and E. A. Adler, June (1980).
- PPG-497 "The Firehose Instability in a Magnetotail Geometry," J. E. Maggs, July (1980).
- PPG-498 "Magnetohydrodynamic Stability of High-Beta Closed-Line Systems," P. L. Pritchett, July (1980).
- PPG-499 "Magnetohydrodynamic Origin of Crab Nebula Radiation," C. F. Kennel and F. S. Fujimura, July (1980).
- PPG-500 "Ultrarelativistic Electromagnetic Pulses in Plasmas," M. Ashour-Abdalla, J. N. Lebeouf, T. Tajima, J. M. Dawson, and C. F. Kennel, July (1980).
- PPG-501 "A CW Far Infrared Laser Scattering Apparatus for Plasma Wave Studies," W. A. Peebles, N. C. Luhmann, A. Mase, H. Park, A. Semet, August (1980).
- PPG-502 "Ion Plasma Waves in a Non-Neutral Plasma," Guy Dimonte, August (1980).
- PPG-503 "Anomalous Absorption of Ordinary Electromagnetic Waves in Magnetized Plasmas," A. Lin and C. C. Lin, August (1980).
- PPG-504 "Finite Length Particle Simulation," P. Liewer, A. Lin, J. M. Dawson, M. Caponi, August (1980).
- PPG-505 "Passive Feedback Stabilization of One Levitated Coil by Means of Super-Conducting Loops," M. Q. Tran, A. Lee, and R. Bowlen, submitted to Journal of Applied Physics, August (1980).
- PPG-506 "Development of 2-D Structure in Cavities," by D. L. Eggleston, A. Y. Wong, and B. C. Darrow, August (1980).
- PPG-507 "Stability of Multipoles to Ballooning Modes with Large Toroidal Mode Number," E. A. Adler and Y. C. Lee, August (1980).
- PPG-508 "San Diego Abstracts, Papers for the San Diego Meeting of the American Physical Society, Division of Plasma Physics," November 10-14, 1980.
- PPG-509 "ICRF Heating in Microtor/Macrotor," R. J. Taylor and G. J. Morales, August (1980).
- PPG-510 "Summary, Conclusions and Recommendations from the Plasma Edge Experiments in Modeling Workshop," A. K. Prinja and R. W. Conn, September (1980).
- PPG-511 "Magnetic Islands Conference and Intense Plasma Heating," C. C. Wu, J. N. Lebeouf, T. Tajima, and J. M. Dawson, submitted to Physical Review Letters, September (1980).
- PPG-512 "Magnetohydrodynamic Particle Code: Lax-Wendroff Algorithm with Finer Grid Interpolations," F. Brunel, J. N. Lebeouf, T. Tajima, and J. M. Dawson, September (1980).
- PPG-513 "Collisionless Shocks & Upstream Waves & Particles: Introductory Remarks," C. F. Kennel, September (1980).
- PPG-514 "Absorbing Boundary Condition and Rudden Turning Point Technique for Electromagnetic Plasma Simulations," T. Tajima and Y. C. Lee, September (1980).
- PPG-515 "Resistivity and Energy Flow in a Plasma Undergoing Magnetic Field Line Reconnection," N. Wild, W. Gekelman, and R. Stenzel, September (1980).
- PPG-516 "Stationary Electrostatic Solitary Waves in the Auroral Plasma," W. Lotko and C. F. Kennel, October (1980).
- PPG-517 "Computer Modeling of RF Heating," V. K. Decyk, G. J. Morales, and J. M. Dawson, October (1980).
- PPG-518 "Microwave Experimental Simulations of Laser-Plasma Interactions," N. C. Luhmann, October (1980).
- PPG-519 "Intra-Granular Helium Gas Behavior in Fusion Reactor Materials," M. I. Takata, N. M. Ghonen, October (1980).
- PPG-520 "Parasitic Instabilities in Efficiency Free Electron Lasers," A. T. Lin, to Physical Review Letters, October (1980).
- PPG-521 "Instabilities of Low Frequency, Parallel Propagating Electromagnetic Waves in the Earth's Foreshock Region," R. D. Sentman, J. P. Edmiston, and L. A. Frank, November (1980).
- PPG-522 "Physics Phenomena in the Analysis of Advanced Fusion Fuel Cycles," G. W. Shuy & R. Conn, August (1980).
- PPG-523 "A Stabilized Axisymmetric Tandem Mirror Plug and Barrier Using Field Reversal," G. W. Shuy, Y. C. Lee, F. Kantrowitz, November (1980).
- PPG-524 "Upstream Hydromagnetic Waves and Their Association with Backstreaming Ion Populations: JSEE 1 & 11 Observations," M. Hoppe, C. T. Russell, L. A. Frank, T. E. Eastman, W. Greenstadt, November (1980).

PPG-525 "Raman Heated Electron Distributions," M. A. Ebrilhim, C. Joshi, H. A. Baldis, November (1980).

PPG-526 "Laboratory Experiments on Magnetic Field Line Reconnection," R. Stenzel, W. Geckelman, N. Wild, November (1980).

